Three Dimensional Simulations of Tsunami Generation and Propagation

Project Representative
Takashi Furumura Earthquake Research Institute, The University of Tokyo

Authors
Tatsuhiko Saito Earthquake Research Institute, the University of Tokyo
Core Research for Evolutional Science and Technology, Japan Science and Technology Agency
Takashi Furumura Earthquake Research Institute, the University of Tokyo

A parallel finite-difference numerical simulation program based on the Navier-Stokes (NS) equations is developed for simulating 3-D tsunami generation and propagation. We can simulate 3-D tsunami propagation over several thousand kilometers using this program, although such tsunami propagation over long distances has usually been conducted based on 2-D simulations. We apply the tsunami simulation program to simulate tsunamis caused by the Kuril Islands earthquake of 13 January 2007. Records calculated using the simulation are in close agreement with tsunami records observed off Hokkaido. Tsunami amplitudes calculated by the 3-D NS equations are smaller than those obtained using the conventional 2-D linear long-wave (LLW) simulation in a direction perpendicular to the fault strike. This is because the 2-D LLW simulation cannot include dispersion effect, and hence the LLW simulation fail to evaluate tsunami amplitude evaluation. The dispersion effect appears during the 2007 off Kuril Island event for which the sea-bottom deformation is restricted to a small area. Our simulation results indicate that the conventional LLW simulation cannot serve as a good approximation to the NS simulation for this event.

Keywords: tsunami, simulation, finite-difference method, Navier-Stokes equations

1. Introduction

Tsunami simulations have been conducted mostly in 2-D space based on the long-wave approximation, instead of solving 3-D Navier-Stokes (NS) equations. Simulations based on the 2-D linear long-wave (LLW) equations are cost effective and widely used for the estimation of the slip distribution along seismic faults or tsunami hazard assessments for past and expected future large earthquakes. Tsunami simulations have also been employed for constructing tsunami databases used for tsunami alert systems such as those operated by the Japan Meteorological Agency (JMA).

Because 2-D simulations employ long-wave approximations and so do not allow calculation of the vertical flow, the tsunami generation process due to the sea-bottom uplifting is not modeled in the 2-D simulations, but given as an initial tsunami height distribution. Numerous 2-D tsunami simulations assume that the initial tsunami-height distribution is identical to the sea-bottom deformation caused by the earthquake [e.g. Satake 1989]. This assumption may be valid for many tsunamigenic earthquakes that occur along the subducting plate and cause deformation of the sea-bottom over a large area. However, a small sea-bottom deformation area would not result in as great an uplift of the sea surface as would occur for the sea-bottom. On the other hand, 3-D tsunami simulation can simulate the tsunami generation process caused by the sea bottom deformation. Furthermore, the 3-D simulation naturally includes a dispersion effect which is neglected in the 2-D LLW equations.

This study develops a parallel simulation program for solving the 3-D NS equations on a large scale in order to simulate tsunami generation and propagation over realistic bathymetry. In the present manuscript, we first give a brief explanation of the NS equations and the numerical technique based on the SOLA method, which was originally proposed by Hirt [1975]. A parallel algorithm and the efficiency of the simulation using a large number of processors are also demonstrated. We, then conduct a 3-D tsunami simulation for tsunami excited by the Kuril Islands (M8.1) earthquake that occurred on Jan. 17, 2007.

2. Navier-Stokes Equations for Tsunamis

The motion of a fluid is described by the following 3D NS equations in Cartesian coordinates (x, y, z),

$$\begin{cases} \frac{\partial u}{\partial t} + u\frac{\partial u}{\partial x} + v\frac{\partial u}{\partial y} + w\frac{\partial u}{\partial z} = -\frac{\partial}{\partial x}\left(\frac{p}{\rho_0}\right) + \nu\nabla^2 u \\ \frac{\partial v}{\partial t} + u\frac{\partial v}{\partial x} + v\frac{\partial v}{\partial y} + w\frac{\partial v}{\partial z} = -\frac{\partial}{\partial y}\left(\frac{p}{\rho_0}\right) + \nu\nabla^2 u \\ \frac{\partial w}{\partial t} + u\frac{\partial w}{\partial x} + v\frac{\partial w}{\partial y} + w\frac{\partial w}{\partial z} = -\frac{\partial}{\partial z}\left(\frac{p}{\rho_0}\right) + \nu\nabla^2 w + g \end{cases} \quad (1)$$

where u, v, and w are velocity components along the x, y, and z- axes, respectively, p is pressure, g is acceleration due to gravity, ρ_0 is the density, and ν is the kinematic viscosity coefficient for water [e.g. Snieder 2001]. The viscosity of water is characterized by a very small value of $\nu = 10^{-6}$ m^2/s.

Assuming incompressible fluid flow, the continuity equation is given by

$$\frac{\partial u}{\partial x} + \frac{\partial v}{\partial y} + \frac{\partial w}{\partial z} = 0. \quad (2)$$

When we take a free surface at rest as $z = H_0$, the bottom is given by $z = h_b = H_0 - h(x, y)$ where $h(x, y)$ is the water depth. The free surface is given by $z = h_s(x, y, t) = H_0 + \eta(x, y, t)$, where $\eta(x, y, t)$ is the fluctuation of the surface at time t. We may consider $\eta(x, y, t)$ as the tsunami. The kinematic boundary condition at the sea surface is given by

$$\frac{\partial \eta}{\partial t} + u\frac{\partial \eta}{\partial x} + v\frac{\partial \eta}{\partial y} = w \ \text{ for } \ z = h_s(x, y, t). \quad (3)$$

These are the equations governing the behavior of water waves, which can be used to describe tsunami generation and propagation.

The deformation of the bottom is directly introduced into the simulation through the water flow at the cell at the bottom. Suppose that the bottom is rising linearly with constant velocity and with final vertical displacement distribution at the bottom after the source process time t_s being given by $d(x, y)$; the corresponding boundary condition at the bottom is then given by,

$$w(x, y, h_b(x, y)) = \begin{cases} d(x, y)/t_s & \text{for} \quad 0 < t \le t_s \\ 0 & \text{for} \quad t > t_s. \end{cases} \quad (4)$$

The vertical flow caused by the bottom deformation results in elevation of the surface. The elevation, or the height distribution at the surface, is propagated as a tsunami.

We use the SOLA technique originally developed by Hirt et al. [1975] to solve above equations and boundary conditions. The NS equations are solved numerically using the FDM with a staggered-grid model.

We develop the parallel program for distant tsunami excited by the bottom deformation and propagating for over one thousand kilometers. The parallel algorithm is based on a traditional domain partitioning procedure, where the 3D model is partitioned horizontally into many subregions with one-cell overlapping of neighbor sub-regions. Each processor calculates the velocity and pressure fields occurring in equations (1)–(4) at each grid point in the assigned sub-region, and a message passing interface (MPI) is used for exchanging data between neighbor sub-regions at each time step.

The parallel tsunami code has been implemented on a cluster of PCs consisting of 16 AMD Opteron processors, (CPU speed 1.4 GHz), connected over a fast Infiniband computer network (communicating at 1 Gb/s), and the Earth Simulator supercomputer. Figure 1 illustrates the results of parallel computing in terms of faster execution of the computation using a large number of CPUs. A fairly good improvement in speed and thus a reduction in elapsed time for the 3-D tsunami simulation is found with increasing processor numbers from 2, 4, to 8 for a smaller simulation model of 512 × 204 × 512 grid points, which takes computer memory of about 3 GBytes when using double-precision arithmetic. However, parallel computing using more processors (16) does not result in good performance with the present simulation model. This is because of the overhead of the MPI communication between large numbers of processors relative to the total computation time of the NS equations of the divided model. Good parallel performance with increasing computational speed using a large number (16) processors is confirmed for a large simulation model of 512 × 204 × 1024, which required computer memory of about 6 GB.

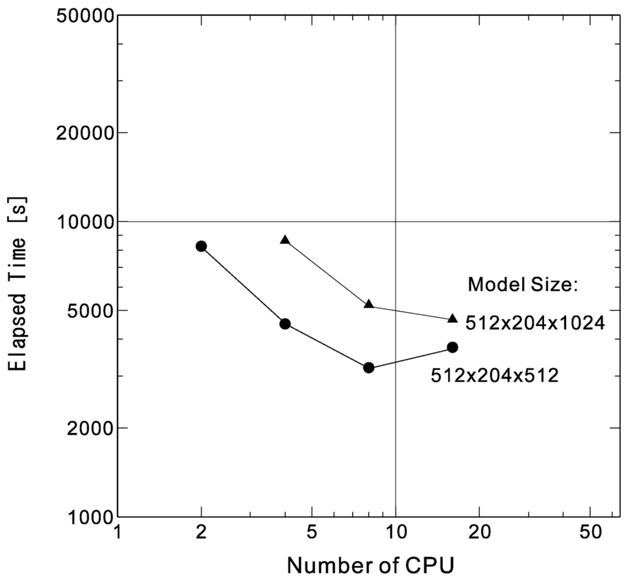

Fig. 1 Parallel performance of the parallel 3D Navier-Stokes simulation in terms of the elapsed time of the tsunami simulation as a function of CPU numbers, and for different scales of the simulation model.

The tests demonstrate the effectiveness of the parallel FDM simulation for solving 3-D NS equations using large number of processors. Care is needed to match the appropriate number of processors to the scale of the simulation model in order to ensure good parallel performance.

3. Tsunami Simulations of the 2007 off Kuril Islands Earthquake

3.1 Tectonic settings around the Kuril Islands

The Kuril Islands form an island arc associated with the subducted Pacific plate underneath the North American plate, and the Kuril trench is more than 8000 m deep. The seismicity around this area is very active and M8-class earthquakes have occurred repeatedly between the two plates. On January 13 2007, a large M8.1 earthquake occurred off the Kuril Islands. This earthquake was a normal-fault event with a steep dip angle (60°), occurring within the subducting Pacific plat and was classified as an intraplate event. The Japan Meteorological Agency (JMA) warned of the arrival of large tsunami more than 3 m high at the coast of eastern Hokkaido and over 2 m high along the Pacific coast of Honshu, Japan. However, the observed tsunami from the earthquake was very weak - less than about 0.5 m high along the Pacific coast of northern Honshu, Japan.

3.2 Tsunami Simulations based on the Navier-Stokes equations

We simulate the tsunamis of the 2007 off Kuril Islands event based on the 3-D NS equations. The area of the simulation model was 1600 km by 2048 km horizontally, and extended to a depth of 22 km, which is discretized into 1600 × 2048 × 110 grid points with a uniform mesh size of 1 km in horizontal directions and 0.2 km in depth. Digital bathymetric data of ETOPO2 provided by the consortium of NOAA, NESDIS, and NGDC was employed in the simulation.

The fault model was derived from the analysis of far-field seismogram data by Ji [2007]. Referring to this model, we set parameters for a constant slip model on a flat fault plane. The top depth of the fault was 4 km and the fault sizes were 200 km and 35 km in the strike and dip directions, respectively. The focal parameters were given by dip = 58°, strike = 45°, rake = –90°. The total seismic moment was $M_0 = 1.9 \times 10^{21}$ Nm, and the source process time was about 70 s. The static deformation of the sea bottom caused by the earthquake was calculated by using a method of Okada [1992] where an analytical expression of the static deformation of an elastic half space is given.

Snapshots of tsunami propagation from the 2007 Kuril Islands earthquake are illustrated in Fig. 2 at times 1, 35, 70, and 105 min from the earthquake origin time. In the first frame of the snapshot (t =1 min), generation of a tsunami with large subsidence and small uplift caused by the normal-fault event is clearly seen; the maximum subsidence of the tsunami above the source zone is approximately –2 m, while the maximum uplift is 0.4 m. In the second frame of the snapshot at a lapse time of 35 min, the tsunami shows clear directivity; a large tsunami is propagating in the direction perpendicular to the fault strike whereas a small tsunami is traveling in the direction parallel to the fault strike. A faster propagation of

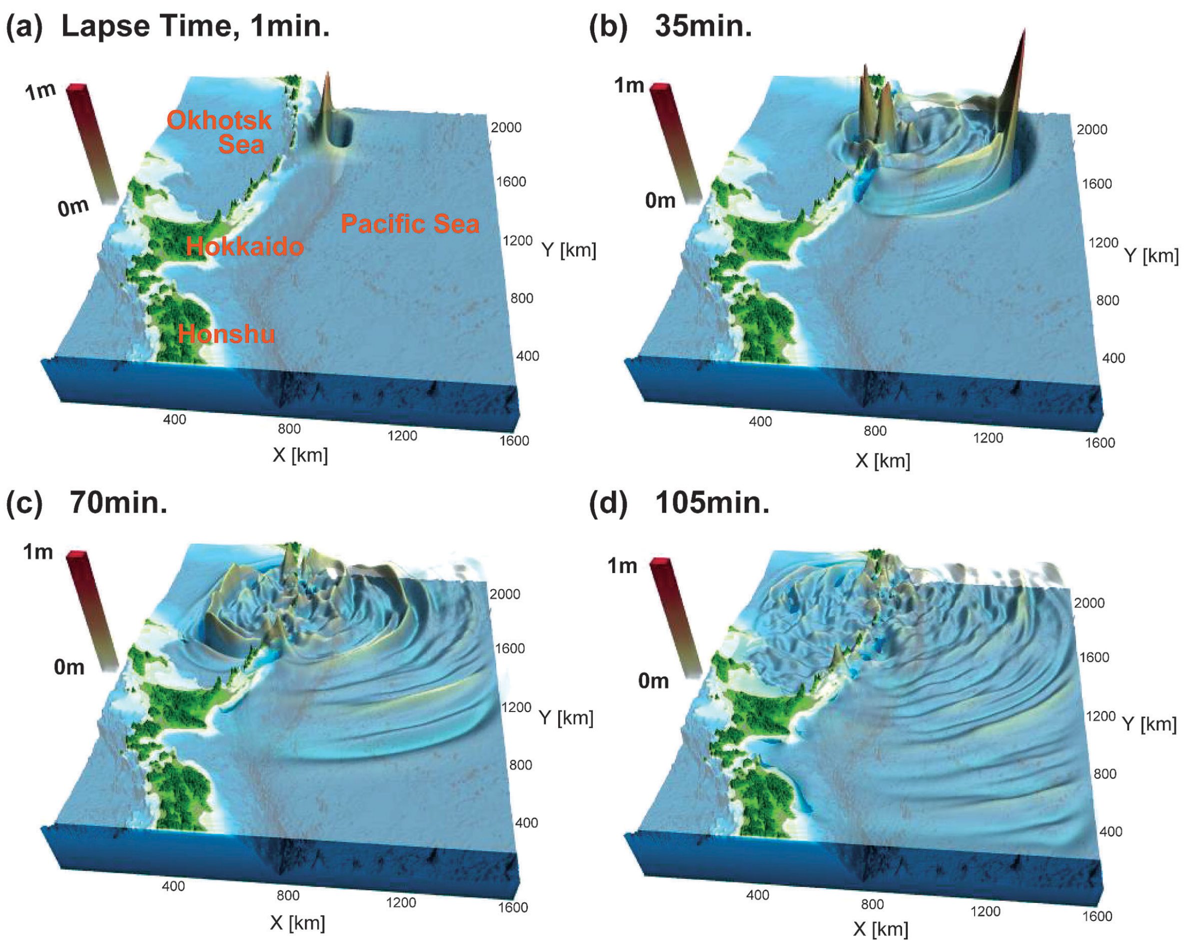

Fig. 2 Snapshots of the tsunami propagation for the Kuril Island earthquake in 2007, at lapse times of (a) 1 min, (b) 35 min, (c) 70 min, and (d) 105 min from the earthquake origin time. These snapshot results are simulated using a model based on the 3-D NS equations.

tsunami in the deep ocean (h > 8000 m) along the Kuril trench at a velocity of approximately 250 m/s arrives at Hokkaido after about 60 min as a small-amplitude head wave. The tsunami propagates slowly in the Okhotsk sea (~140 m/s), which is shallow (h ~ 2000 m). At a lapse time of 70 min, the leading tsunami characterized by subsidence is arriving at the Pacific coast of Hokkaido. At later times, trapping of the scattered tsunami near the source region and in the shallow sea surrounding the Kuril Islands is evident.

3.3 Comparison of Simulations based on the Navier-Stokes and Linear Long-Wave Equations

The results of tsunami derived from the NS and linear long-wave (LLW) simulations are compared in Fig. 3 using snapshots of tsunami propagation at an elapsed time of t = 40 min. There is a significant difference between the two results; the dispersion of tsunami propagation in the direction perpendicular to the fault strike (along the x-axis) can be clearly seen from the NS simulation [Fig. 3]. The wave train is developed near the wave front due to the dispersion in the deep ocean. The dispersion of tsunami traveling in the deep ocean results in long-wavelength leading tsunamis in the NS simulation. On the other hand, the LLW simulation shows a simple impulsive leading wave in this direction since the LLW simulations cannot include the dispersion effect due to the long-wave approximation.

The tsunami records calculated by the two methods are compared in Fig. 4. The simulated tsunami shows strong dispersion in the NS simulation and it forms a wavetrain. In contrast, the tsunami in the LLW simulation shows no dispersion and a sharp leading wave. The calculated tsunami records were compared with the observed record off Kushiro, located about 1000 km from the source region [point K in Fig. 3]. The Japan Agency for Marine-Earth Science and Technology (JAMSTEC) operates bottom-pressure gauges offshore of Kushiro at a depth of 2200 m. The gray line in Fig. 4 for station K illustrates the observed tsunami at the offshore station. At the beginning of the observed record at a time before 20 min, a large-amplitude high-frequency seismic wave arrives, and then large and long-period tsunami at periods of approximately 30 min arrive near a time of 60 min. Solid and dashed lines shown in Fig. 4 for station K indicate the tsunami derived from the NS and LLW simulations, respectively. We used $M_0 = 9.5 \times 10^{20}$ [Nm] (Mw 7.9) both in the NS and LLW simulations. Both calculated traces are plotted 2.5min later to fit the record. Although a slight discrepancy is found in phases later than 85 min, the tsunami records calculated using the two simulations show no significant differences around the main part of the tsunami. This is mainly because there was negligible dispersion apparent in this direction.

4. Discussion and Conclusions

A parallel FDM program for simulating long distance tsunami based on the 3-D NS equations has been developed for accurate representation of a tsunami source caused by sea bottom deformation and propagation over the deep ocean. Long distance tsunami propagating more than a thousand kilometers has been simulated by parallel computing using a large number of processors. Such large scale simulations have usually been conducted based on 2-D long-wave theory where the initial tsunami height distribution is often assumed to be identical to the sea bottom deformation caused by the earthquake.

NS simulation has been conducted for the tsunami result-

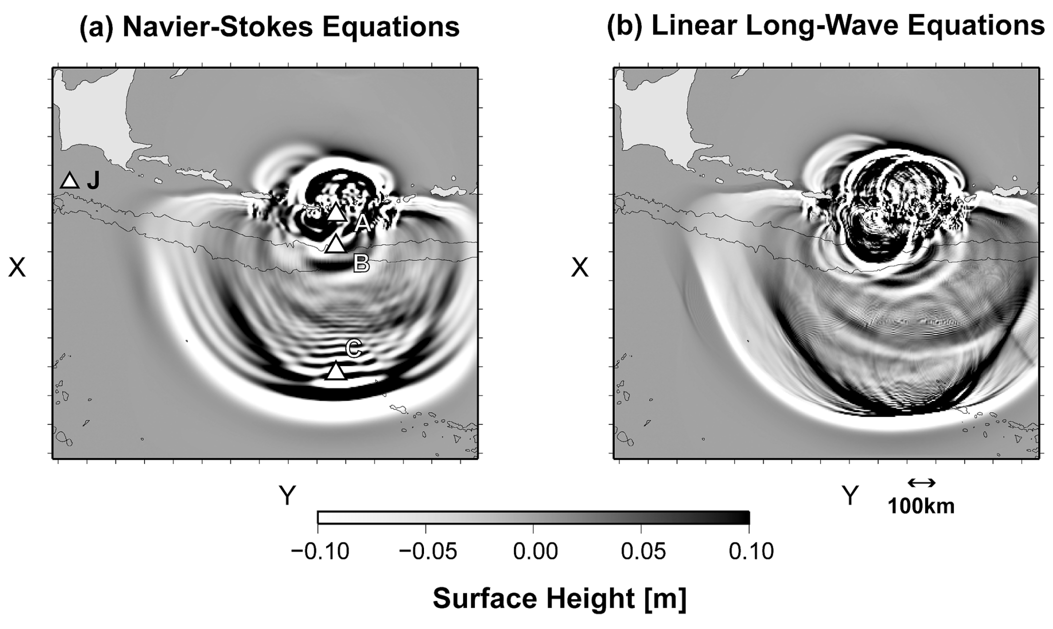

Fig. 3 Surface height distribution at a lapse time t = 40 min from the earthquake origin time calculated from the (a) NS and (b) LLW simulations.

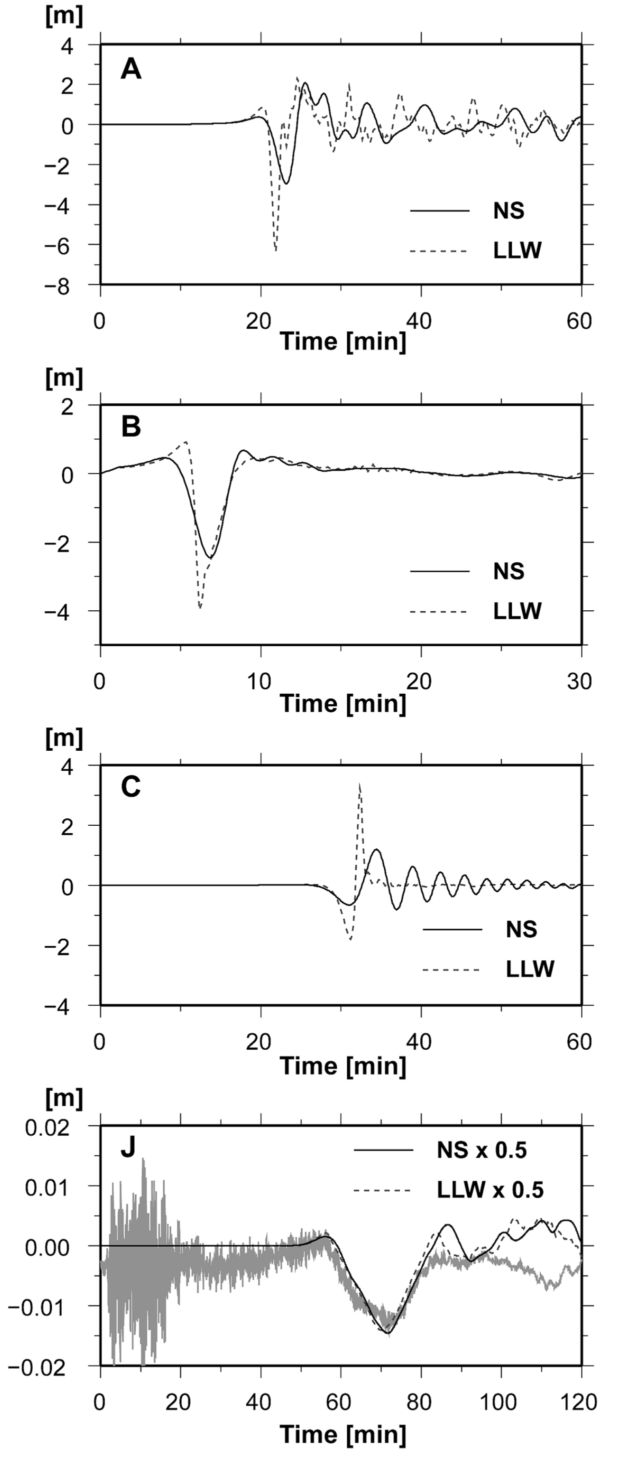

Fig. 4 The tsunami record calculated from the simulation using the NS equations (solid curve) and the LLW equations (dashed curve), at stations A, B, C and J shown in Fig. 3. At station J, calculated tsunami records are multiplied by 0.5 to compare with the tsunami record (gray line) observed off Tokachi (marked J in Fig. 3).

ing from the Kuril Islands event (M8.1) of January 13, 2007, which occurred in the subducting Pacific plate at a depth h ~ 6000 m. The steeply dipping normal-fault of this interplate earthquake produced a large subsidence (~ –5 m) at the sea bottom within a small area of 40 km in width and 200 km in length. We have confirmed that the 2-D LLW simulation did not serve as a good approximation to the 3-D NS simulation for the 2007 Kuril event. The maximum tsunami amplitude calculated by the LLW simulation was larger than that of the NS simulation around the source area and in the direction perpendicular to the fault strike. However, we were not able to find any significant differences between the tsunami records off Hokkaido calculated from the two simulation methods.

The tsunami alert of JMA warned that larger tsunami more than 3 m high would attack the Pacific coast of Japan during this event, but the observed tsunami were several times smaller than the JMA estimation. There were two possible reasons for this overestimation of tsunami height before the above analysis; the first arising from overestimation of the JMA magnitude, and the second resulting from inappropriate use of long-wave simulation. The results of our tsunami simulations show that the differences between the NS and the LLW simulations were only minor for the Pacific coast of Japan. Therefore, we guess that incorrect estimation of the JMA magnitude was the main reason for the overestimation of the tsunami height at the Kuril event. In any case, further analysis is needed to clarify why a tsunami alert was mistakenly issued for the 2007 Kuril event.

Acknowledgements

We used records from the bottom-pressure gauge operated by the Japan Agency for Marine-Earth Science and Technology (JAMSTEC). This study was supported by a grant-in-aid from the Core Research for Evolutional Science and Technology (CREST), the Japan Science and Technology Agency. This study was conducted by a joint research project between the Earthquake Research Institute, University of Tokyo and The Earth Simulator Center, JAMSTEC entitled “3D simulation of seismic wave propagation in heterogeneous structure”.

References

Hirt, C. W., B. D. Nichols, and N. C. Romero (1975), SOLA - A numerical solution algorithm for transient fluid flows, Los Alamos National Laboratory report LA-5852.

Ji, C. (2007), USGS Earthquake Center, http://earthquake.usgs.gov/eqcenter/

Okada, Y. (1992), Internal deformation due to shear and tensile faults in a half-space, Bull. Seismol. Soc. Am. 82, 1018–1040.

Satake, K. (1989), Inversion of tsunami waveforms for the estimation of heterogeneous fault motion of large submarine earthquakes: the 1968 Tokachi-oki and 1983 Japan Sea earthquakes, J. Geophys. Res. 94, 5627–5636.

Snider, R. (2001), A Guide Tour of Mathematical Method, Cambridge university press, Cambridge.

津波生成と伝播の3次元数値シミュレーション

プロジェクト責任者
古村　孝志　　東京大学　地震研究所

著者
齊藤　竜彦　　東京大学　地震研究所
　　　　　　　科学技術振興機構　CREST
古村　孝志　　東京大学　地震研究所

流体運動は3次元ナヴィエ・ストークス式（NS式）で記述されるが、津波発生および伝播過程は、津波波長が十分長いと仮定し、2次元線形長波方程式に基づきシミュレートされる場合が多い。これに対し、本研究では3次元NS式に基づき、長波近似を用いることなく津波発生・伝播過程をシミュレートする並列計算プログラムを開発した。並列計算を行うことで、1000km以上もの長距離を伝播する津波をシミュレートすることが可能となり、実際に観測される津波記録への高い適用性をもつ。これを利用し、2007年1月13日に千島列島沖で発生した地震による津波をシミュレートした。震源からおよそ900km離れた釧路沖で観測された津波記録の特徴を、開発したプログラムによって高精度に再現できることを確認した。さらに、これまでの代表的な津波シミュレーション法である2次元線形長波方程式によるシミュレーションの結果と比較することで、長波近似の適用性について吟味した。3次元NSシミュレーションでは、地震断層の走行に直行する方向で、津波の分散が顕著に現れるのに対し、2次元線形長波シミュレーションではこの特徴を再現することはできない。この違いは、2007年千島列島沖地震が高角度の傾斜角度をもつプレート内部地震であったために、海底変動面積が狭く、長波近似の適用範囲を超えていることに起因する。つまり、2次元線形長波方程式は必ずしも3次元NS式の良い近似とはならず、高精度な津波モデリングのためには3次元NS式に基づいたシミュレーションが必要となる。

キーワード：津波, シミュレーション, 差分法, Navier-Stokes方程式